You might find this additional information useful...

This article cites 53 articles, 22 of which you can access free at:
 http://ajprenal.physiology.org/cgi/content/full/295/4/F959#BIBL

Updated information and services including high-resolution figures, can be found at:
 http://ajprenal.physiology.org/cgi/content/full/295/4/F959

Additional material and information about *AJP - Renal Physiology* can be found at:
 http://www.the-aps.org/publications/ajprenal

This information is current as of January 10, 2010 .

The molecular and functional phenotype of glomerular podocytes reveals key features of contractile smooth muscle cells

Moin A. Saleem,[1] Jiri Zavadil,[2] Maryse Bailly,[5] Karen McGee,[5] Ian R. Witherden,[1] Hermann Pavenstadt,[4] Hsianghao Hsu,[4] Julia Sanday,[1] Simon C. Satchell,[1] Rachel Lennon,[1] Lan Ni,[1] Erwin P. Bottinger,[2] Peter Mundel,[3] and Peter W. Mathieson[1]

[1]*Academic and Children's Renal Unit, University of Bristol, Southmead Hospital, Bristol, United Kingdom;* [2]*Albert Einstein Biotechnology Center and* [3]*Department of Anatomy and Structural Biology, Albert Einstein College of Medicine, Bronx, New York;* [4]*Universitätsklinikum Münster, Münster, Germany; and* [5]*Division of Cell Biology, UCL Institute of Ophthalmology, London, United Kingdom*

Saleem MA, Zavadil J, Bailly M, McGee K, Witherden IR, Pavenstadt H, Hsu H, Sanday J, Satchell SC, Lennon R, Ni L, Bottinger EP, Mundel P, Mathieson PW. The molecular and functional phenotype of glomerular podocytes reveals key features of contractile smooth muscle cells. *Am J Physiol Renal Physiol* 295: F959–F970, 2008. First published August 6, 2008; doi:10.1152/ajprenal.00559.2007.— The glomerular podocyte is a highly specialized cell, with the ability to ultrafilter blood and support glomerular capillary pressures. However, little is known about either the genetic programs leading to this functionality or the final phenotype. We approached this question utilizing a human conditionally immortalized cell line, which differentiates from a proliferating epithelial phenotype to a differentiated form. We profiled gene expression during several time points during differentiation and grouped the regulated genes into major functional categories. A novel category of genes that was upregulated during differentiation was of smooth muscle-related molecules. We further examined the smooth muscle phenotype and showed that podocytes consistently express the differentiated smooth muscle markers smoothelin and calponin and the specific transcription factor myocardin, both in vitro and in vivo. The contractile contribution of the podocyte to the glomerular capillary is controversial. We demonstrated using two novel techniques that podocytes contract vigorously in vitro when differentiated and in real time were able to demonstrate that angiotensin II treatment decreases monolayer resistance, morphologically correlating with enhanced contractility. We conclude that the mature podocyte in vitro possesses functional apparatus of contractile smooth muscle cells, with potential implications for its in vivo ability to regulate glomerular dynamic and permeability characteristics.

mesenchyme; smoothelin; epithelial-mesenchymal transition; differentiation; development

THE RENAL GLOMERULUS IS COMPOSED of a complex microcirculation, arranged in a network of capillary loops supported by the interstitial mesangium. Podocytes are highly specialized cells in the renal glomerulus and form a major part of the filtration barrier, preventing protein loss (predominantly albumin) in the urine. A distinct architectural feature of podocytes is their interdigitating foot processes, which enmesh the glomerular capillary loop, with the formation of a unique cell-cell junction termed the slit diaphragm (34). In addition, the podocyte needs to withstand, and possibly respond to (32), the high capillary pressures generated in the glomerulus, adding to its need for specialized cellular apparatus (30). There is controversy in the literature, however, over the contractile role of podocytes beyond regulation of slit size (20), and the mesangial cell has been postulated as providing the tensile role within the glomerulus, on the basis of cytoskeletal observations (8).

The unique molecular apparatus utilized by the podocyte in defining its functions has recently begun to be elucidated, aided in large part by the identification of genes mutated in congenital nephrotic syndromes (4, 22, 43) and the development of in vitro tools to study function (31, 41).

Traditionally the podocyte has been described as an epithelial cell type (in fact, an alternative name used is the glomerular visceral epithelial cell). Developmentally, however, there is an observational change from simple epithelial cells during the S-shaped body stage to a mature mesenchymal phenotype, with reexpression of vimentin and loss of epithelial markers such as desmosomal proteins and E-cadherin and of proliferation markers (12, 31). The extent and nature of this change is unknown and will be important in predicting how the mature podocyte behaves in vivo. These questions were addressed by utilizing a human conditionally immortalized cell line that mimics many of these changes during in vitro differentiation (41). In the differentiated state, the immortalizing SV40 gene is inactive so is more representative of the in vivo phenotype. We have studied in vitro the developmental transition in the podocyte, as it changes from a proliferating, simple epithelial phenotype to a mature differentiated cell. We describe, initially using a gene array approach in conditionally immortalized human podocytes, that there is early genetic programming, including upregulation, unexpectedly, of certain genes associated with smooth muscle differentiation. To elaborate on this, we show that mature podocytes express specific proteins associated with a differentiated smooth muscle phenotype and have vigorous contractile properties, modulated by angiotensin II (ANG II). This has delineated in detail some markers associated with the differentiated podocyte and shows that this cell has a unique differentiation profile including smooth muscle features, which may be important in its ability to maintain the glomerular microcirculation and ultrafiltration characteristics.

METHODS

Cell Culture

A human conditionally immortalized podocyte cell line was generated and cultured as described (41). Cells were allowed to proliferate at 33°C and grown to 80% confluence in 180-cm² flasks. This was designated *day 0*. For subsequent time points, cells were thermoswitched at *day 0* to 37°C, which caused inactivation of the SV40 T antigen, and cessation of cell replication could be observed within 24 h. Cells were harvested and RNA prepared at *days 0*, *3*, *9*, and *12* [cells are fully differentiated by *day 14* (41)]. For biological triplicates, separate flasks were used, at the same conditions and time points, and the RNA prepared from these was hybridized independently to microarray chips.

K562 control cells were used as the internal standard for microarray (an erythroleukemia human cell line) and were grown in suspension in the above medium, at 37°C, and harvested at a density of $4-6 \times 10^5$/ml.

Rat A7R5 aortic smooth muscle cells (SMCs) were obtained from the American Type Culture Collection (Bethesda, MD). Human mesangial cell primary cultures were a kind gift of Professor A. O. Phillips, University of Cardiff, Wales. NIH 3T3 cells were obtained from European Collection of Animal Cell Cultures (Porton Down, UK).

Preparation of RNA

RNA was extracted from cultured cells using the Trizol method (23), and 100 μg of podocyte RNA was prepared for hybridization to each microarray chip, along with 100 μg of RNA from K562 control cells.

Microarray

For every time point (*days 0*, *3*, *9*, and *12*), 100 μg of podocyte RNA + 100 μg control RNA was hybridized per microarray chip, and three independent repeats were performed at each time point (i.e., 300 μg podocyte RNA at each time point). The microarray chips used were Human H6 gene chips, containing 9,216 unique sequences (Albert Einstein School of Medicine, Biotechnology Center).

Hybridization, normalization and data filtering, and quantitative PCR analysis were performed as previously described (55). Statistically significant differential mRNA abundance across time points was established by significance analysis of microarrays (www-stat-class.stanford.edu/) software applying a 1% false discovery rate (FDR) (45). Data is submitted in the NCBI repository (GEO, http://www.ncbi.nlm.nih.gov/geo/), accession number GPL961.

qPCR

Quantitative real-time RT-PCR (qPCR) was performed by use of the ABI Prism 7900 Sequence Detection System. Podocyte RNA was converted into cDNA with Superscript II reverse transcriptase (Invitrogen/BRL, Carlsbad, CA). Gene-specific sequences for PCR primers were designed to generate amplicons of 50–100 base pairs required for quantitative real-time detection, by using SYBR Green Master Mix (Applied Biosystems, Foster City, CA). The mRNA abundances were determined by normalization of the data to the expression levels of GAPDH or β_2-microglobulin mRNA.

Immunofluorescence

The immunolabeling was done as previously described (31). Antibodies were obtained as follows: Nephrin monoclonal antibody 43C7 was a kind gift of Prof. Karl Tryggvason, Stockholm, Sweden; smoothelin monoclonal C6G was a kind gift of Prof. G. van Eys, University of Maastricht, Netherlands; anti-mouse myocardin antibodies A1043a and A1043b were from Antibody Core, UT Southwestern at Dallas, TX; monoclonal anti-calponin, smooth muscle myosin, and α-SMA were all purchased from Sigma (St. Louis, MO).

Samples used were either human podocytes grown at 33°C (undifferentiated) or for 14 days at 37°C (fully differentiated), or a specimen of normal adult donor kidney unused for renal transplant (with institutional ethical approval). For human kidney, 5-μm sections were fixed, washed, and blocked as for cells, with an additional step of 15% glacial acetic acid for 15 min and 0.3% hydrogen peroxide for 15 min. Newborn mouse kidney sections (C57 black) were a gift of Dr. Rommel Ravanan (University of Bristol, Veterinary School). Antibody conjugation and mounting were as above. Standard images were obtained via a Leica photomicroscope attached to a Spot 2 slider digital camera (Diagnostic Instruments) and were processed with Adobe Photoshop 5.0 software.
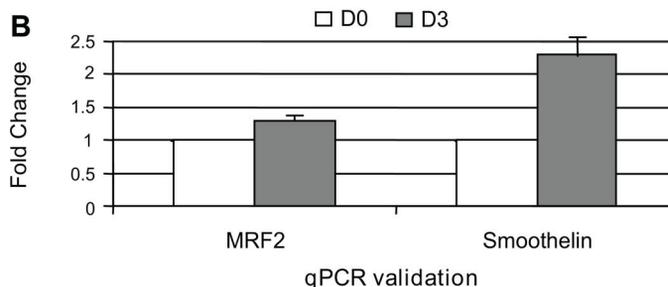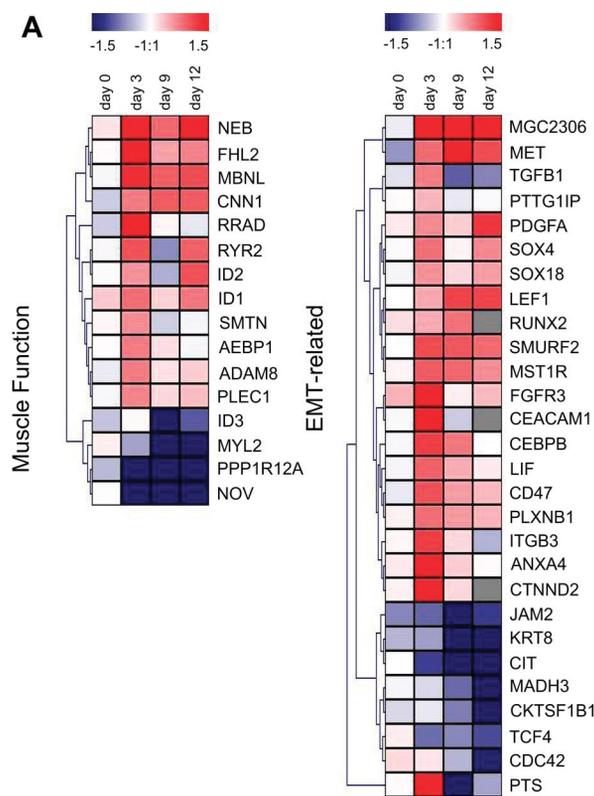

Fig. 1. Microarray analysis and quantitative PCR (qPCR). *A*: identification and functional classification of regulated genes during podocyte differentiation. Cluster diagrams show expression profiles (based on median ratios normalized against baseline) of regulated genes in two related functional categories, representing 44 of 458 regulated genes. Color spectrum bars indicate upregulation (red) or downregulation (blue) with fold change of expression from −1.5 to +1.5. Gene name abbreviations correspond to Unigene nomenclature. *B*: quantitative PCR expression of smoothelin and MRF2. Time points analyzed were *day 0* (proliferating cells at 33°C) and *day 3* after thermoswitching. *Day 0* (D0) shows a normalized median ratio of gene of interest expression to GAPDH expression, and *day 3* (D3) indicates the fold change of expression compared with baseline (3 repeats). Error bars indicate SE.

Western Blotting

Total cell lysates were prepared for Western blotting by addition of a lysis buffer containing 1% saponin to cells, and methods used were as previously described (41).

Cell Contractility

Single cell elastomer wrinkling assay. Cells were trypsinized and replated onto deformable elastomer substrates as described by Wrobel et al. (52). The flexibility of the substratum permits the contractile forces exerted by the cells to be measured without affecting cytoskeletal expression (17). Podocyte contractility was assayed by blinded counting of the number of wrinkles generated per cell in the surrounding elastomer substrate at 4 h after seeding, in a minimum of nine fields of view (20 cells per view, minimum), in three separate experiments. Statistical values were obtained by Mann-Whitney *U*-test using the SPSS statistical package.

Collagen contraction assay. Cell-embedded collagen matrixes to measure contraction were made following a modification of a previously described protocol (11). Briefly, 150 μl of a collagen solution containing 1.5 mg/ml collagen (First Link) and 2.6×10^5 cells/ml gel in cell culture medium were cast in the 14-mm central microwell of 35-mm Mattek dishes (Mattek). The gels were polymerized for 15–30 min at 37°C and then manually detached from the edge of the wells. Excess unpolymerized solution was aspirated and 2 ml of medium supplemented with 10% FCS was added. For experiments involving angiotensin stimulation, the gel mix was prepared with serum-free medium and 2 ml of serum-free medium was added to the gel after polymerization. The cells in gels were starved for 2 h prior to stimulation with 100 nM ANG II (Sigma), with or without prior incubation with the inhibitors for 30 min (losartan 100 nM, PD123349 10^{-5} M, both Sigma).

Whole gel contraction was monitored by digital images taken immediately following release of the polymerized gels (*time 0*) and then daily for 7 days, or at 2, 8, and 22 h for the angiotensin assay. Images were imported into Image J software, and the gel area was measured with reference to the outline of the well. The contraction was calculated as the percentage change from the original surface.

Direct contraction force monitoring was done by using our previously described SIM-CFM (simultaneous imaging and culture force monitor) (11) on a humidified, CO_2-regulated epifluorescent microscope stage (Zeiss). Force measurements were recorded in 3-ml collagen matrixes seeded with either 3.3×10^6 cells/ml of undifferentiated podocytes or 1×10^6 cells/ml of differentiated podocytes. Force readings recorded by Picolog (Pico Technology) and Xware 6.0.4 (Parker Software) were obtained every second over a 15-h period after the matrixes were cast. The temperature was kept constant throughout the experiment, 33°C for undifferentiated podocytes and 37°C for differentiated podocytes. Net contractile force was calculated by subtracting the baseline force measurements obtained from matrixes free of cells and correcting the resulting value to obtain net force per million cells.

Time course analysis of podocyte monolayer resistance in response to Ang II. Time course analysis and resistance modeling was performed using an automated cell monitoring system, electrical cell-substrate impedance sensing (ECIS 1600R, Applied Biophysics, Rochester, NY), which can detect nanometer-order changes of cell-to-cell and cell-to-substrate distances separately (21). The instrument applies a small alternative current (<1 μA at 4,000 Hz) between two electrodes using culture medium as the electrolyte. The instrument monitors both the amplitude and phase of the signal and from this information reports the impedance, resistance, and capacitance of the small electrode treating the system as a simple resistive capacitative series circuit. The source of impedance has been shown to be due both to the constricted current flow in the spaces beneath the basal membrane and the surface of the electrode and to the resistance in the paracellular path between adjacent cells (19). Briefly podocytes were seeded on to gold microelectrodes in wells of ECIS arrays (8 well, 10+ electrodes per well) and allowed to differentiate at 37°C for 14 days. Nonconfluent cell monolayers were treated with ANG II 5×10^{-8} M (Sigma Chemical) ± preincubation for 30 min with losartan (Merck) or vehicle control in serum-free medium. By use of the ECIS attachment mode, resistance was measured at regular time intervals from the point of addition of substrate, for up to 90 min. The ratio of measured resistance to baseline resistance was calculated for each well and plotted as a function of time, normalized to control.
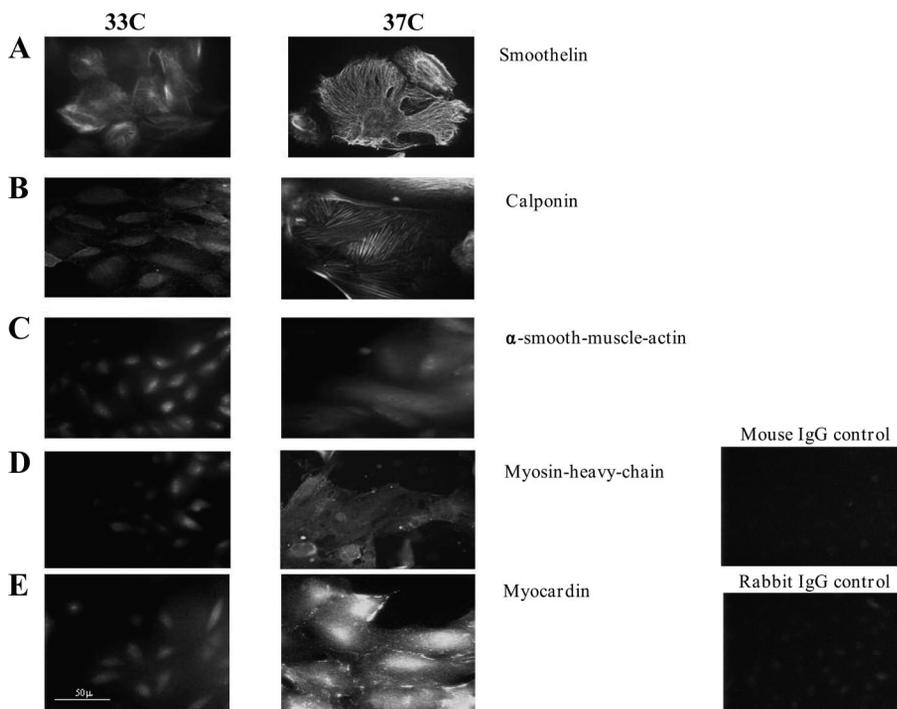

Fig. 2. Cellular immunofluorescence (all comparative images were taken at the same exposure; control IgG staining is shown at *right*). Smoothelin, myocardin, and calponin antibodies were raised in mouse, smooth muscle myosin, and α-smooth muscle actin (SMA) antibodies were raised in rabbit. *A*: smoothelin, showing faint filamentous expression in undifferentiated cells, and typical, strong filamentous distribution in differentiated cells. *B*: calponin. Faint, diffuse expression in undifferentiated cells; strong expression in differentiated cells in a pattern of actin stress fibers. *C*: α-SMA. Nuclear expression is nonspecific compared with negative control (not shown). Some cytoplasmic expression is seen and appears slightly stronger in differentiated cells. *D*: myosin heavy chain. No significant expression above negative control (not shown) in undifferentiated cells, with positive expression in differentiated cells. *E*: myocardin. No significant expression above control (not shown) in undifferentiated cells; strong nuclear and some cytoplasmic expression in differentiated cells. Magnification ×400.

In nonconfluent cell layers resistance measurements are related to the fractional area of the electrodes occupied by cell cytoplasm and can therefore be used as an indirect measurement of changes in cell morphology (contraction or relaxation) (21). Comparisons in cell culture experiments were made by repeated-measures ANOVA with post hoc Bonferroni analysis. Results are presented as means ± SE.

Response of podocytes to ANG II and inhibition of both AT1 receptors (losartan) and AT2 receptors (PD123319, Sigma) was also tested in the gel contraction assay. For these experiments cells were used between passages 17 and 21 and differentiated for 11–17 days. The graph shown (Fig. 7C) is average of three experiments for losartan and two for PD123319. Each experiment is in triplicate, with the resulting controls for serum free and ANG II being for 7 experiments (both pooled). Shown are means ± SE. Angiotensin and losartan were both 100 nM, and PD123319 was 10^{-5} M.

RESULTS

All gene name abbreviations correspond to Unigene nomenclature.

During Differentiation, 5% of Genes Are Regulated at a 99% Level of Confidence

Examining 9,216 unique expressed sequences, we identified 458 significantly regulated transcripts (FDR 1%), with expression data normalized for *day 0*. Regulated gene data was distributed into hierarchical gene clusters, by use of TIGR multiple experiment viewer software (http://www.tigr.org), and genes of known function were classified according to LocusLink
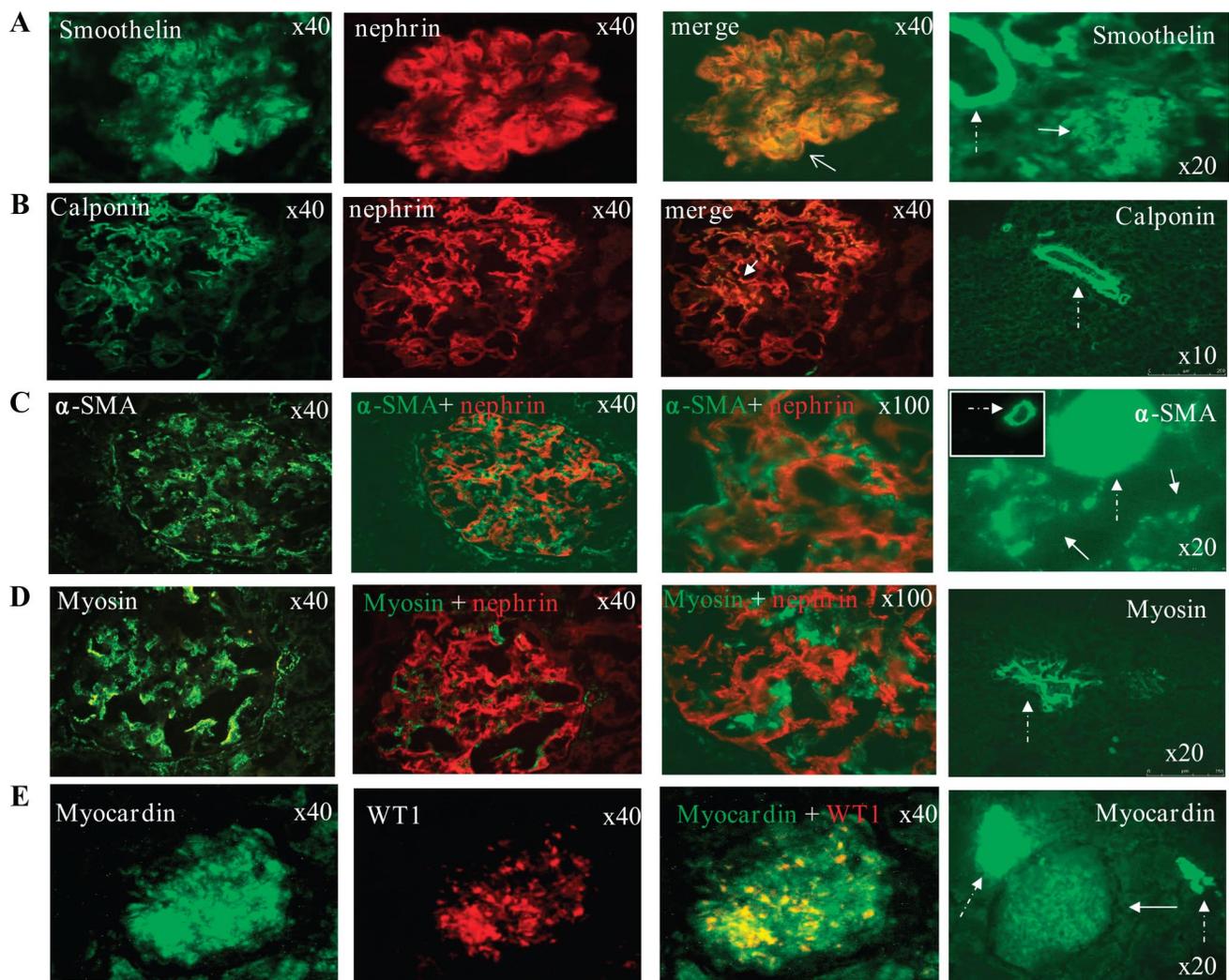

Fig. 3. Glomerular immunofluorescence. *A*: smoothelin (green). *Left*: linear, capillary loop pattern. *Center*: nephrin staining (red). *Right*: double immunostaining with nephrin demonstrating colocalization (yellow, arrow shows an example in a capillary loop). *B*: calponin (green). *Left*: linear, capillary loop pattern. *Center*: nephrin staining (red). *Right*: double immunostaining with nephrin demonstrating colocalization (yellow, arrow shows an example in a capillary loop). *C*: α-SMA (green). *Left*: mesangial cell pattern of distribution, with relatively weak podocyte staining. *Center*: double immunolabeling with nephrin to localize podocytes (red). *Right*: the same at higher magnification, demonstrating absence of colocalization. *D*: myosin heavy chain (green). *Left*: mesangial cell pattern of distribution, with relatively weak podocyte staining. *Center*: double immunolabeling with nephrin to localize podocytes (red). *Right*: the same at higher magnification, demonstrating absence of colocalization. *E*: myocardin (green). *Left*: nuclear cell staining. *Center*: WT-1 staining (a nuclear podocyte marker). *Right*: double staining with WT-1 colocalizing with myocardin (yellow). Magnification ×40 to ×100. Far right-hand column shows the level of expression of each protein in vascular smooth muscle in the same sections, illustrating greater level of expression compared with glomeruli. Where a glomerulus is present in the same panel, this is indicated by the solid arrow. Stippled arrows indicate blood vessels. For SMA (*C*), the *inset* is the same view as the main panel and shows the same artery, at lower fluorescence intensity.

(http://www.ncbi.nlm.nih.gov/LocusLink/) and Gene Ontology (http://www.geneontology.org/).

Among Genes Expressed in Differentiation, a Revealing Subgroup Is of Genes Involved in Smooth Muscle Differentiation

We were surprised to find early (*day 3*) upregulation of 16 genes specifically associated with SMC differentiation and function (Fig. 1*A*). This included genes coding for nuclear proteins associated with SMC phenotype switching (*ID1*, *ID2*, *ID3*), a sarcomeric muscle protein (*sarcosin*), a gene coding for a calcium release channel in muscle contraction (*RYR2*), genes involved in terminal differentiation of muscle cells (*FHL2*, *MBNL*), vascular smooth muscle development (*ADAM8*, *AEBP1*), and cytoskeletal contractile function (*SMTN*, *CNN1*, *NEB*, *PLEC1*). Of these, smoothelin (*SMTN*) was of particular interest, being a molecule expressed solely in fully differentiated contractile smooth muscle (46). Smoothelin gene upregulation was confirmed by qPCR on *days 0* and 3 (Fig. 1*B*). In keeping with the switch to a more mesenchymal phenotype during differentiation, we report also the appropriate upregulation/downregulation of 28 epithelial-mesenchymal transition-related genes which were not further examined in this study (Fig. 1*A*).

To further support a smooth muscle differentiation pathway, we confirmed by qPCR the consistent early expression of the SMC differentiation gene *MRF2* (49) (not present on the array chip), in cultured differentiating cells (Fig. 1*B*). We also validated by qPCR expression patterns of selected genes from each clustered group (smoothelin is shown as an example, Fig. 1*B*).

We then examined the expression of smoothelin and calponin (*CNN1*) at the protein level using immunofluorescence and Western blotting (Figs. 2–5), showing expression of calponin, and both "visceral" (59 kDa, also known as smoothelin-A) and "vascular" (110 kDa, also known as smoothelin-B) isoforms of smoothelin (25) in differentiated podocytes. Interestingly, the vascular isoform was upregulated in differentiated cells (Fig. 5*B*). The immunofluorescence (IF) appearance of smoothelin was filamentous in podocytes, consistent with the observation that in some cell types it has a filamentous distribution (46) and in others it is stress fiber associated (7). The antibody we used has been used to detect human smoothelin transfected into COS7 cells (46), yielding the same IF distribution. Calponin had the typical stress fiber distribution in cultured podocytes (Fig. 2*B*). In human glomerular sections, double stained with the podocyte marker nephrin, both proteins were found specifically in podocytes (Figs. 3, *A* and *B*). Expression of smoothelin in podocytes was noticeably weaker than in arteriolar SMCs in the same sections. We further examined the smooth muscle phenotype of undifferentiated and differentiated podocytes by examining other known myofibroblastic markers: smooth muscle myosin heavy chain (MHC) and α-smooth muscle actin (SMA) (Figs. 2 and 5). There was expression of SMA by IF and Western blotting in vitro and no detectable expression by IF of MHC at 33°C, with expression at 37°C. Weak nuclear staining of SMA was also seen in vitro, compared with control, of uncertain significance. MHC and SMA were detected strongly in a mesangial cell distribution in vivo, with comparatively weak podocyte expression (Fig. 3).
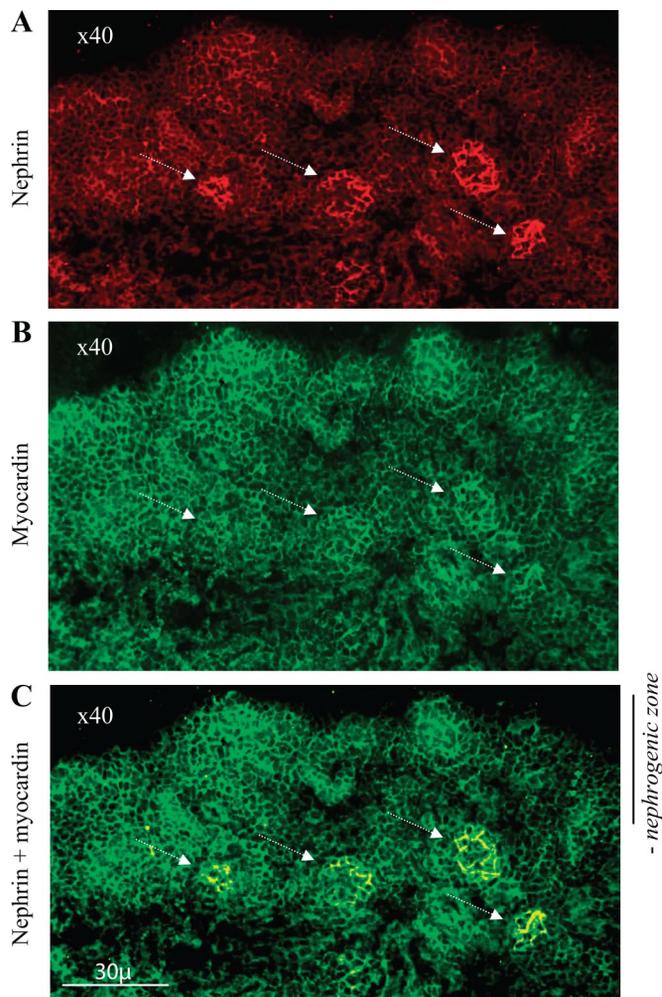

Fig. 4. Expression of myocardin in developing newborn mouse glomeruli. *A*: nephrin. Showing expression of nephrin in mature glomeruli (stippled arrows) deep in the cortex (nephrin is expressed in postcapillary loop stage glomeruli), whereas more immature glomeruli in the subcapsular "nephrogenic zone" show no significant expression. *B*: myocardin. Definite expression is seen in only mature glomeruli. *C*: merged image, showing colocalization (yellow) in podocytes in the mature glomeruli.

Podocytes Express Myocardin in Vitro and In Vivo

Myocardin is a cardiac- and smooth muscle-specific cofactor for the ubiquitous transcription factor serum response factor (SRF). Gain- and loss-of-function experiments have shown myocardin to be sufficient and necessary for SMC differentiation (47), although a subsequent study noted that the full repertoire of SMC genes is not controlled by myocardin (53). Consistent with our observations here, myocardin has recently been shown to regulate the smoothelin promoter, via SRF (39). Thus it was important to demonstrate the presence of this factor in differentiated podocytes (the gene was not represented on the array chip). Using two separate antibodies, we demonstrated the presence of myocardin. Undifferentiated cultured podocytes showed very low nuclear expression compared with the nonspecific control IgG (Fig. 2*E*). Differentiated cells showed nuclear expression, as well as a distinct stippled cell membrane and cytoplasmic distribution (seen consistently with both antibodies); the likelihood is that this factor shuttles between cytoplasm and nucleus upon serum activation (Fig.

Fig. 5. Western blotting of smooth muscle proteins. *A*: SMA expression in differentiated (*lane 1*) podocytes. Positive and negative controls: stronger expression in a smooth muscle cell line (*lane 2*) and very weak expression in HK2 epithelial cells (*lane 3*). *B*: smoothelin. Indicates the predominantly visceral isoform of smoothelin (59 kDa) in colon control (*lane 1*); HK2 epithelial cell negative controls are shown in *lane 2*. Both contractile (110 kDa) and visceral isoforms seen in undifferentiated cells (*lane 3*). Differentiated cells show an upregulation of the contractile isoform, whereas the visceral isoform is unchanged (*lane 4*). *C*: myocardin. Colon positive control (*lane 1*); HK2 tubular epithelial cells negative control (*lane 2*); undifferentiated podocytes (*lane 3*); and differentiated podocytes, slightly greater expression (*lane 4*). *D*: calponin Western blot. Increased expression (34 kDa) in differentiated podocytes (*lane 2*) compared with undifferentiated podocytes (*lane 1*); glomerular extract (glom; *lane 3*) colon positive control (cont; *lane 4*), and very weak expression in HK2 cells (*lane 5*).

A Smooth Muscle Actin

B Smoothelin

C Myocardin

D Calponin
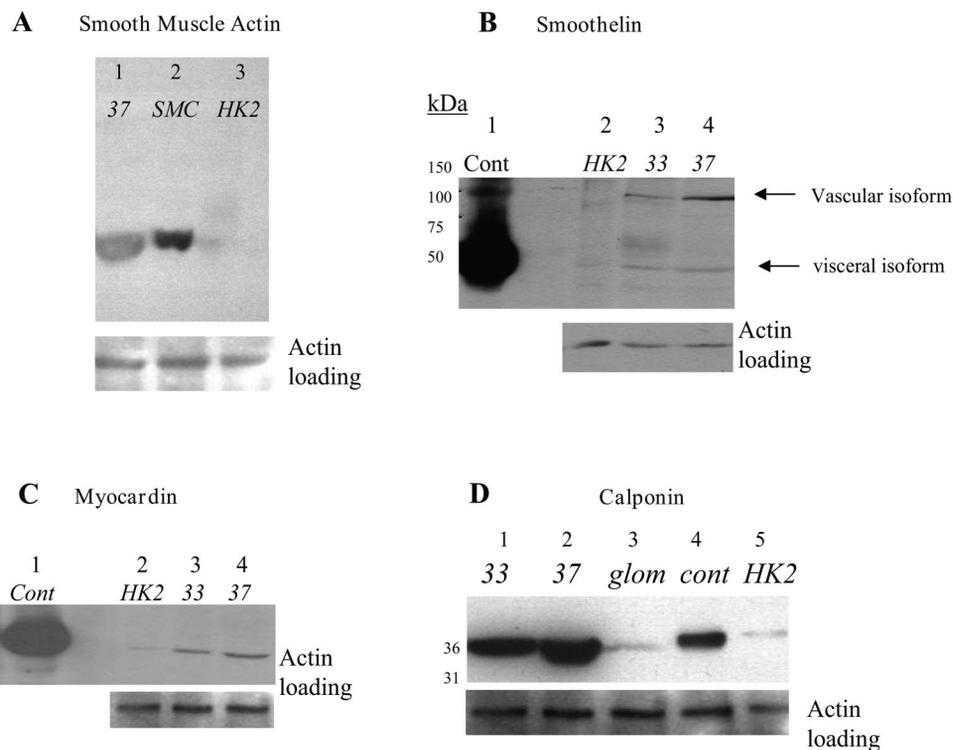
2*E*). On Western blotting a distinct band at ~60 kDa was seen, in undifferentiated and differentiated cells (Fig. 5*C*). In glomerular sections, nuclear expression of myocardin was seen with both available anti-myocardin antibodies, and this expression mainly colocalized with WT1 as a podocyte nuclear marker, although we did not rule out the possibility of additional expression in mesangial cells (Fig. 3*E*). Of note, the expression levels of myocardin in podocytes compared with "professional" SMCs in arterioles in the same sections were lower, suggesting differential regulation.

Next, we examined the appearance of myocardin in developing podocytes by looking at expression in newborn mouse kidney, which displays glomeruli at different stages of development from S-shaped body through capillary loop stage to mature glomeruli (28). Myocardin was seen to be coexpressed with nephrin in morphologically mature glomeruli. There was also myocardin expression in the subcapsular nephrogenic zone, where more immature glomeruli are located (S-shaped bodies), where nephrin is not yet expressed, although it is not clear which structures this expression corresponds to (Fig. 4).

Podocytes Contract Vigorously Once Differentiated, in an Actin-Dependent Manner

Because we observed evidence of a smooth muscle contractile apparatus, we decided to functionally examine the ability of podocytes to contract in vitro. We applied two recently developed techniques to examine contractility. The first quantifies single cell contractility and was originally used in fibroblasts when they acquire a myofibroblastic morphology (52). The technique has been validated by using measurements of single cell force generation and appears to correlate very well with the appearance of wrinkles counted on a silicon gel. Differentiated podocytes produced 6.71 ± 0.3 wrinkles/cell after 4 h, compared with 4.4 ± 0.2 wrinkles/cell for undifferentiated podocytes ($n = 9$ fields), and both were significantly greater than 3T3 fibroblasts, which generated 0.04 ± 0.01 wrinkles/cell ($P < 0.001$). The results showed a highly significant increase in contractility between undifferentiated podocytes or fibroblasts and differentiated podocytes (Fig. 6*B*).

Fig. 6. Collagen matrix contraction assay. *A*: single cell contractility after 4 h on substrate; appearance of wrinkles on substrate indicates cell contraction: (*i*) undifferentiated NIH3T3 fibroblasts, no wrinkles; (*ii*) undifferentiated podocytes showing few, short wrinkles; (*iii*) differentiated podocytes showing multiple deep, long wrinkles on silicon elastomer; (*iv*) rat aortic smooth muscle control, multiple deep wrinkles. *B*: graphs showing single-cell contractility measured by counts of substrate wrinkles per cell. Bars show median, interquartile range, and highest and lowest values. Statistical analysis used the Kruskal-Wallis test. *P < 0.05. *C*: gel contraction assay. Representative confocal reflection image of gel (*left*) and differential interference contrast (DIC) image (*right*) of undifferentiated cell on *day 3* after seeding. Note the alignment of the matrix toward the cell (also visible in the DIC image). *D*: gel contraction assay. Cell contraction measured by percentage of gel area. Undifferentiated podocytes contract 3D collagen gels over 7 days down to ~20% of the original gel area. Differentiated podocytes have much more vigorous contractile properties, reaching maximal contraction within the first 24 h after seeding in the gel. Control NIH3T3 fibroblasts show similar contraction kinetics as undifferentiated podocytes (error bars indicate mean contraction percentage at each time point $\pm$ SE). *E*: gel contraction assay. Force generation during matrix contraction. Undifferentiated and differentiated podocytes were seeded in collagen matrixes at a density of 3.3×10^6 and 1×10^6 cells/ml, respectively, and placed on the culture force monitor system. Force associated with matrix contraction was recorded every second for ~15 h. The graph shows the baseline-corrected mean force generated by 10^6 cells for each cell type. Values shown are means and SE from 4 experiments.

The second technique measures cell contractility within a 3D matrix and records the ability of a cell type to contract a collagen matrix within which cells have been seeded (11). The results were consistent with the first technique and showed highly vigorous contractility of differentiated podocytes, compared with undifferentiated podocytes or NIH 3T3 fibroblasts (which were not significantly different from each other in this instance, Fig. 6D). Direct measurement of force generated by the cells during matrix contraction (Fig. 6E) revealed that the maximal force generated by the differentiated podocytes at plateau stage (around 20 dyn/10^6 cells) was significantly higher than that of the proliferating cells (7 dyn/10^6 cells), actually

A

(i)

(ii)

(iii)

(iv)

C

B

Contractility of different cell types

D

- ◆ Undifferentiated podocytes
- ■ Differentiated podocytes
- ▲ NIH3T3 fibroblasts

Force generation during collagen gel contraction

E
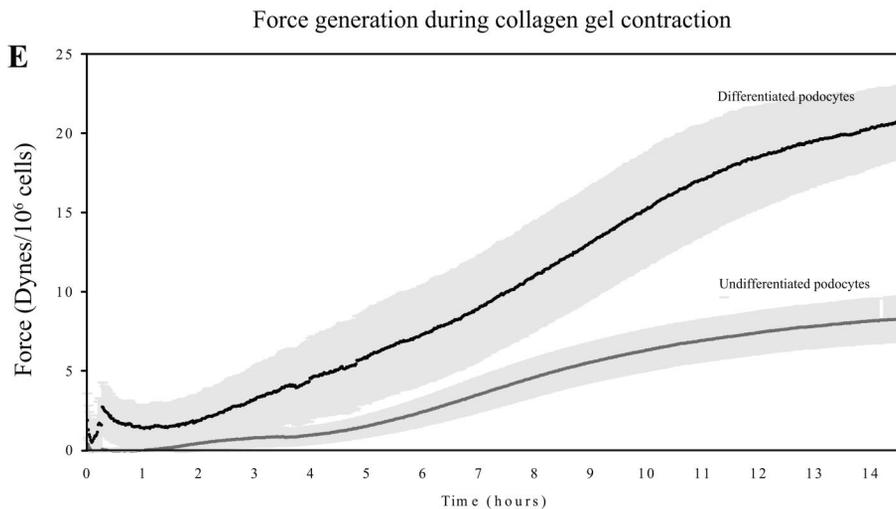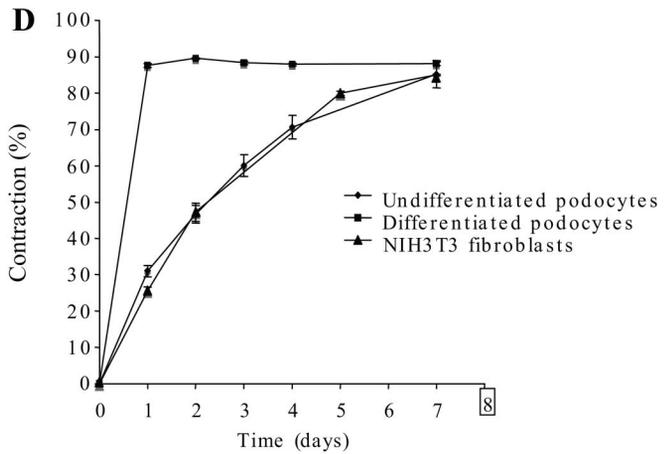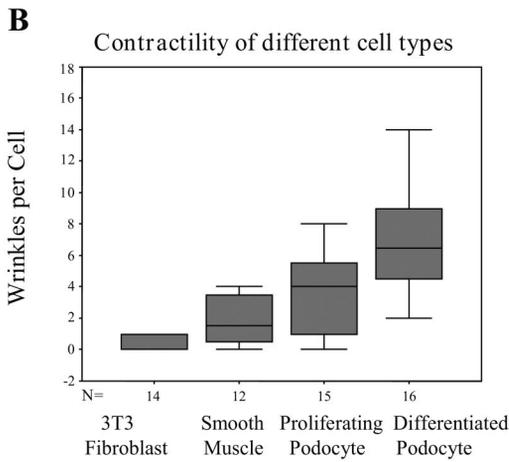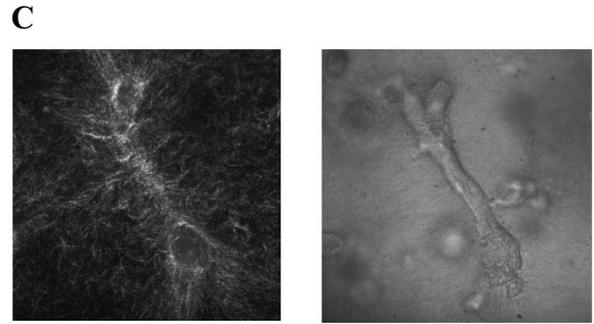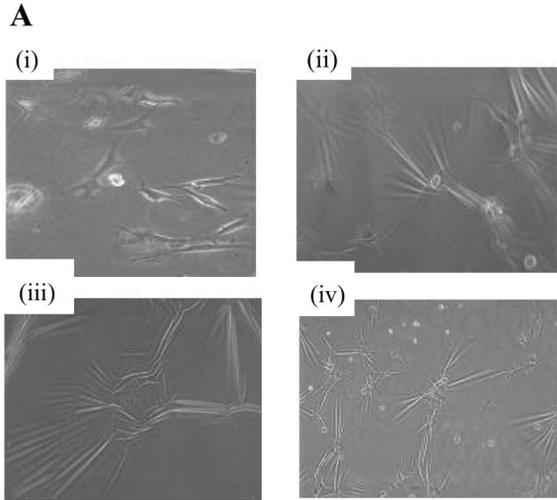
being the same order of magnitude as the force recorded for primary corneal fibroblasts, the most contractile cells so far tested in this system (11).

Podocytes Change Their Shape and Resistance in Response to ANG II

ANG II is a vasoactive agent with the ability to increase smooth muscle tone and myocardial contractility. Because angiotensin-converting enzyme inhibitors have an important function in affecting both glomerular blood flow and attenuating proteinuria, we felt it was important to assess whether ANG II might have a direct effect on podocyte contractility. Firstly we observed morphological changes in podocytes by light microscopy at several time points after stimulation with ANG II and blindly counted contracted cells (Fig. 7A). This revealed visible contraction of cells within 0.5–1 h, which could be quantitated by blinded counting, and was prevented by preincubation with the ANG II receptor blocker losartan.

Using the ECIS system, we were able to quantify at a single cell level the response to ANG II in real time (Fig. 7B). The system allows measurement of resistance averaged across 10 electrodes per well (4 replicate wells per experiment) covered with subconfluent differentiated podocytes, which infers nanometer scale changes in cell shape. The changes in cell shape could be due to changes in cell adhesion, or contraction, and taken in conjunction with the gel assays suggest that the changes measured are at least partly due to podocyte contractility.

The results consistently show a reduction in measured resistance by ANG II within the first few minutes of exposure, which is completely blocked by preincubation with losartan. This indicates cell contraction in response to ANG II that is supported by the morphological observations.

To confirm that ANG II could directly promote a contractile phenotype in the differentiated cells, we tested the response to ANG II in the gel contraction assay. ANG II stimulation led to a significant increase in macroscopic gel contraction compared with serum-free medium, consistent and complementary to the data showing increased contraction on ECIS and by morphology (Fig. 7C). This contractility could be significantly inhibited at the 2- and 7-h time points by both AT1 inhibition (losartan) and AT2 inhibition (PD123319).

DISCUSSION

This study, utilizing a human podocyte cell line, is the first detailed in vitro description of the human podocyte phenotype comparing undifferentiated with differentiated cells and has revealed some novel insights. In particular, we have shown that the mature podocyte in vivo and in vitro displays distinct features of smooth muscle differentiation. This is consistent with an emerging picture of human podocyte biology that suggests

functional analogies with SMCs, such as rapid insulin-sensitive glucose uptake (10, 26) and the recent finding of functional TRPC6 calcium channel expression, which is normally expressed in brain and SMCs (18, 38, 50), with knockout causing enhanced vascular smooth muscle contractility and elevated systemic blood pressure (14).

Podocyte Differentiation Starts From an Epithelial Phenotype

Our previous data on this podocyte cell line indicates that during temperature-induced differentiation the cells change from an epithelial morphology to a phenotype resembling the mature phenotype, with expression of cell cycling- and podocyte-specific antigens that reflect this change (41). This may reflect the developmental stage of glomerulogenesis, at which time the podocyte acquires its final phenotype from a proliferating epithelial precursor in the capillary loop stage (42), and we surmised that the in vitro changes may be studied, with similar genetic programs. This is supported by our observations of more robust and mature expression of slit diaphragm proteins in the differentiated cells (9, 40, 41). A potential limitation in vitro is that differentiation is not complete, and there may be as yet undefined signals that podocytes need in vivo, for example from adjacent cells, to complete the process. Nevertheless, this is the best representative model and fulfils many of the requirements.

Mature podocytes in vivo clearly have some epithelial characteristics, such as basement membrane production and cytokeratin expression. However, they also express vimentin and lose E-cadherin expression suggestive of mesenchymal transformation, and the cell-cell junction (slit diaphragm) is a highly specialized structure unique to this particular cell (37), with a lack of desmosomes or a classical adherens junction. We hypothesized that differentiating podocytes would display some features of epithelial phenotype but also some specialized features that could reflect their reacquisition of mesenchymal features.
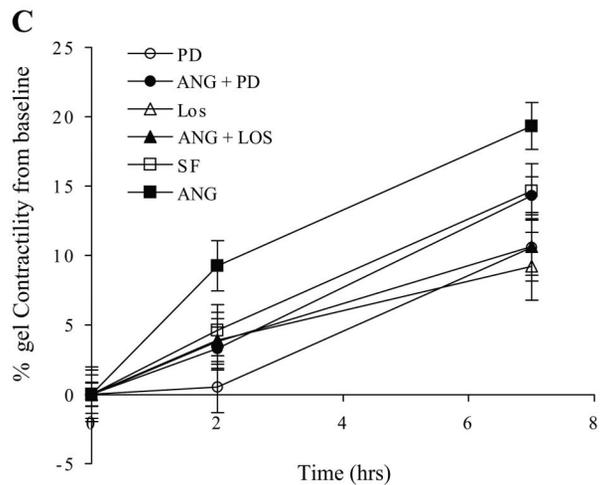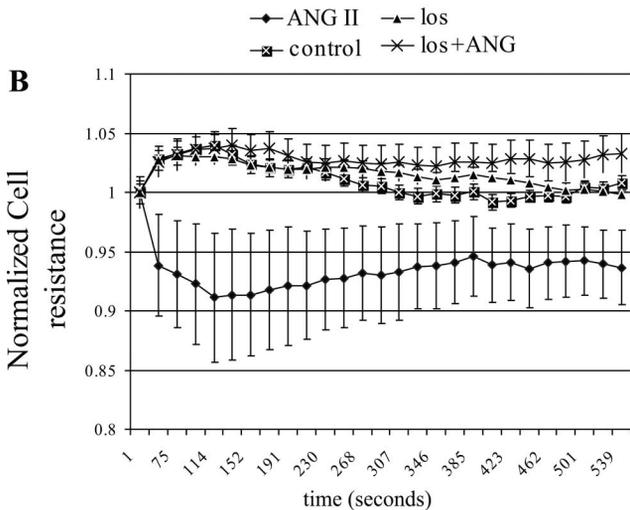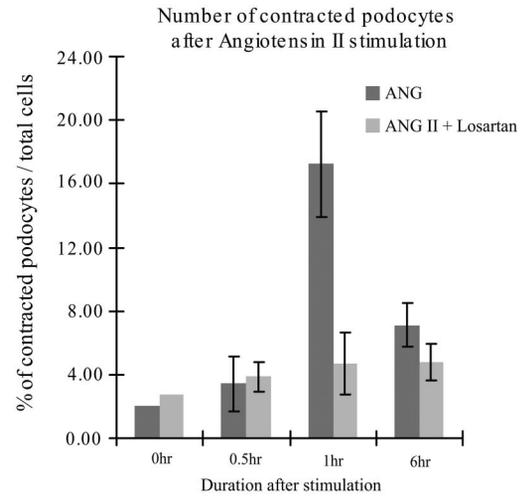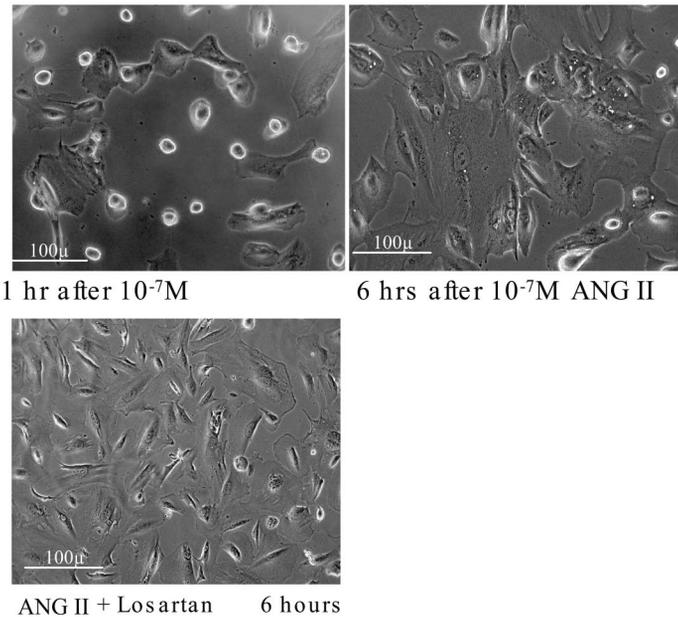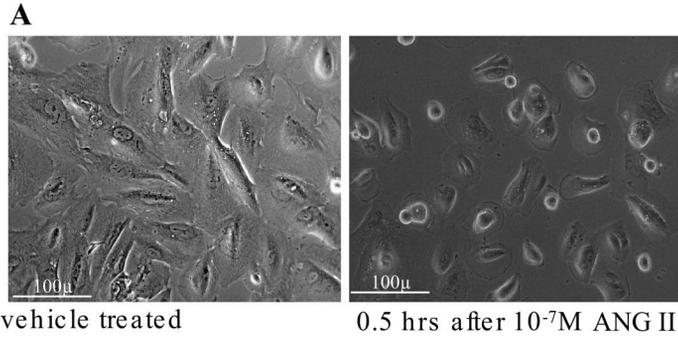
A Distinct Set of Smooth Muscle-Specific Genes Is Upregulated During Differentiation

A striking finding was the number of genes associated with muscle development and function, and in particular specialized smooth muscle differentiation. As one would expect, there are some (though not many) genes expressed that are associated with epithelial phenotype (e.g., keratins). However, we found certain genes that are associated with highly differentiated smooth muscle, such as smoothelin. This is a gene that is reported to be specific for contractile SMCs and not SMC-like cells such as myofibroblasts and is a marker for the end stage of SMC differentiation (46). Expression of smoothelin isoforms seems to be strictly controlled with respect to cell type

Fig. 7. Podocyte contractility in response to angiotensin (Ang) II on differentiated podocytes. A: morphological changes in podocytes by light microscopy at several time points after stimulation with Ang II, and blocking of contraction changes by losartan (Los). Graph shows quantification of contracted cells by blinded counting (3 independent experiments; error bars indicate means ± SE). B: electrical cell-substrate impedance sensing (ECIS). Time course measurement of resistance of differentiated podocytes after Ang II stimulation, and blocking of effect by losartan. Error bars indicate means ± SE. C: angiotensin stimulates cell-mediated gel contraction by differentiated podocytes. Differentiated podocytes were embedded in collagen gels in cell-free medium and starved for 2 h prior to stimulation with Ang II. AT1 inhibitor losartan and ATII inhibitor PD123319 (PD) were added to the medium 30 min prior to stimulation. Shown are means ± SE for 3 experiments done in triplicate for losartan and twice for PD123319. There is no statistical difference between the values of the medium alone (SF) and all others except Ang II (Ang; $P = 0.01$). Significant difference between Ang II (2 and 7 h) and Ang II + PD ($P = 0.003$) or Ang II + Los ($P = 0.01$, Student's t-test).

and developmental stage and may be related to the mode of contraction of different cells (13). Smoothelin is postulated to modify contraction by interacting with actin (33); recently a targeted smoothelin knockout mouse model confirmed a role

for smoothelin in intestinal SMC contractility (33). We looked at other recognized molecular markers of smooth muscle, including α-SMA, smooth muscle MHC, and calponin. Of these, interestingly, calponin was the protein found to be the

A

vehicle treated

0.5 hrs after 10^{-7}M ANG II

1 hr after 10^{-7}M

6 hrs after 10^{-7}M ANG II

ANG II + Losartan   6 hours

Number of contracted podocytes after Angiotensin II stimulation

B

C

most highly expressed in differentiated podocytes, both in vitro and in vivo (and is also upregulated on the array, CNN1). Its expression in SMCs is specifically associated with a contractile cell phenotype, which is lost in noncontractile SMCs (51). Both smoothelin and calponin appear to play a direct role in cell contractility in vivo. In intact smooth muscle from mice with a basic calponin knockout, isometric force is significantly reduced (44).

In differentiated cultured podocytes the expression of α-SMA is upregulated but diffuse in distribution compared with conventional myofibroblasts. This is likely to represent a unique expression profile of α-SMA in podocytes. The expression of α-SMA and smooth muscle MHC in the glomerulus was seen predominantly in the mesangium. Thus in the glomerulus the relative expression of SMA in mesangial cells is stronger than podocytes, whereas smoothelin, calponin, and myocardin are more podocyte specific. The mechanism for this could lie in the differential regulation of α-SMA and smoothelin by myocardin, which was recently elucidated (39). The relative expression levels of smooth muscle proteins in podocytes appears to be unique, with low levels of SMA and myosin compared with smoothelin and calponin. It may be that this is related to control of the unique cytoskeletal composition of podocytes, with foot processes relying on actin for their morphological phenotype. For example, smoothelin is now recognized as interacting with actin for contractile functionality (34), and it may be that foot process contraction and retraction utilize distinct mechanisms.

Finally, to support smooth muscle specificity, we demonstrated in podocytes in vivo and in vitro the expression of myocardin, a transcription factor identified as a regulator of smooth muscle gene expression that, via the ubiquitous SRF, conveys smooth muscle specificity to its target genes and thus appears to be both sufficient and necessary for smooth muscle differentiation (48, 54). We observed both nuclear and cytoplasmic expression of myocardin in vitro, which could be analogous to the nuclear shuttling of related transcriptional family members such as megakaryoblastic leukemia-1 (MKL1), which like myocardin also binds to SRF (6).

The contractile role of podocytes in the glomerulus is controversial. We were able to demonstrate functional contractility in differentiated cells using a recently published method that is able to quantify cell-mediated 3D matrix contraction and also by sensitive cell impedance sensing.

The time courses of these experiments are governed by the kinetics of the experimental method. For example the gel contraction relies on macroscopic contraction, which occurs over hours or days, whereas ECIS impedance measurements are able to detect contraction changes much more rapidly. Rapid response may indicate an ability to counteract pulse pressure dynamically, but further work would be needed to demonstrate this property physiologically.

Are Podocytes a Form of Microvascular Pericyte?

Expression of SMC markers, and the association of podocytes with the glomerular microcirculation, suggests a closer than previously appreciated analogy with pericytes. Pericytes are perivascular cells associated with capillaries and postcapillary venules. Since pericytes have some features of SMCs [with expression of α-SMA, and absence of smooth muscle myosin (3)] and since SMCs are absent from these microvessels, it has long been proposed that pericytes are their contractile counterparts. It has been further considered that pericytes have the capacity for narrowing capillaries and hence regulating microvascular blood flow (1), and recently, central nervous system capillary diameter has been shown to be controlled bidirectionally by neurotransmitters acting on pericytes (35).

Capillary pressures have been estimated at up to 60 mmHg in the human glomerulus (5), approximating to arteriolar pressures, and therefore it has been assumed that the afferent arteriole controls pressures within the glomerulus. In fact it was recently demonstrated that the kinetic features of the glomerular afferent arteriole allow this vessel to adjust tone in response to changes in systolic pressures presented at the pulse rate. This suggests that the primary function of this mechanism is to protect the glomerulus from the blood pressure power that is normally present at the pulse frequency, rather than the previously held belief that this (arteriolar) myogenic response exists to maintain glomerular capillary pressure constant (27). In fact, the podocyte is more likely to support capillary pressures, preventing capillary expansion and maintaining ultrafiltration (30). This assertion is further supported by our previous report that podocytes possess a functional stretch-sensitive K^+ channel (29), providing functional capability to sensing acute changes in capillary pressure. Physiologically the recently described "subpodocyte space" postulates a role for a rapidly contractile podocyte in control of ultrafiltration direction (32).

Our data suggest the podocyte is capable of relatively rapid contractility (ECIS) and sustainable contraction (gel experiments) and is capable of applying great forces on the matrix upon stimulation (force measurements). The respective physiological roles of these is the subject of speculation. For example, slow contraction may play a part in aiding podocyte motility and/or regulating homeostasis with their environment.

Early research supports a contractile role for podocytes, on the basis of foot processes rich in actin, which results in an increase in open filtration slits when relaxed (2), whereas others have suggested that the mesangial cells possess more appropriate cytoskeletal structure for this purpose (8), but there is little functional information to support either assertion. It has also been shown that mechanical stretch initiates expression of the angiotensin system in podocytes (15) and of disease-associated proteins (16). Our data is more comprehensive in defining the contractile machinery present in podocytes and adds functional evidence; more work is needed to define the effects of contraction on the filtration barrier itself.

The mature podocyte phenotype is clearly more complex than originally envisaged, and there are already compelling data to suggest analogies with neuronal cells (24, 36). In fact our array data was consistent with this and demonstrated the upregulation of certain neuronal transcripts also (data deposited online, see METHODS). However, we have found that certain key components of smooth muscle machinery are also present and functional, which adds to the biological intricacy of this cell.

An SMC-like phenotype for such a central cell of the filtration barrier is a novel concept and provides a rationale for targeting this aspect of podocyte biology therapeutically for antihypertensive (and antiproteinuric) agents.

REFERENCES

1. **Allt G, Lawrenson JG.** Pericytes: cell biology and pathology. *Cells Tissues Organs* 169: 1–11, 2001.
2. **Andrews PM, Coffey AK.** Cytoplasmic contractile elements in glomerular cells. *Fed Proc* 42: 3046–3052, 1983.
3. **Bandopadhyay R, Orte C, Lawrenson JG, Reid AR, De Silva S, Allt G.** Contractile proteins in pericytes at the blood-brain and blood-retinal barriers. *J Neurocytol* 30: 35–44, 2001.
4. **Boute N, Gribouval O, Roselli S, Benessy F, Lee H, Fuchshuber A, Dahan K, Gubler MC, Niaudet P, Antignac C.** NPHS2, encoding the glomerular protein podocin, is mutated in autosomal recessive steroid-resistant nephrotic syndrome. *Nat Genet* 24: 349–354, 2000.
5. **Brenner BM, Troy JL, Daugharty TM.** The dynamics of glomerular ultrafiltration in the rat. *J Clin Invest* 50: 1776–1780, 1971.
6. **Cen B, Selvaraj A, Prywes R.** Myocardin/MKL family of SRF coactivators: key regulators of immediate early and muscle specific gene expression. *J Cell Biochem* 93: 74–82, 2004.
7. **Chambers RC, Leoni P, Kaminski N, Laurent GJ, Heller RA.** Global expression profiling of fibroblast responses to transforming growth factor-beta1 reveals the induction of inhibitor of differentiation-1 and provides evidence of smooth muscle cell phenotypic switching. *Am J Pathol* 162: 533–546, 2003.
8. **Cortes P, Mendez M, Riser BL, Guerin CJ, Rodriguez-Barbero A, Hassett C, Yee J.** F-actin fiber distribution in glomerular cells: structural and functional implications. *Kidney Int* 58: 2452–2461, 2000.
9. **Coward RJ, Foster RR, Patton D, Ni L, Lennon R, Bates DO, Harper SJ, Mathieson PW, Saleem MA.** nephrotic plasma alters slit diaphragm-dependent signaling and translocates nephrin, podocin, and CD2 associated protein in cultured human podocytes. *J Am Soc Nephrol* 16: 629–637, 2005.
10. **Coward RJ, Welsh GI, Yang J, Tasman C, Lennon R, Koziell A, Satchell S, Holman GD, Kerjaschki D, Tavaré JM, Mathieson PW, Saleem MA.** The human glomerular podocyte is a novel target for insulin action. *Diabetes* 54: 3095–3102, 2005.
11. **Dahlmann-Noor AH, Martin-Martin B, Eastwood M, Khaw PT, Bailly M.** Dynamic protrusive cell behaviour generates force and drives early matrix contraction by fibroblasts. *Exp Cell Res* 2007.
12. **Davidson G, Dono R, Zeller R.** FGF signalling is required for differentiation-induced cytoskeletal reorganization and formation of actin-based processes by podocytes. *J Cell Sci* 114: 3359–3366, 2001.
13. **Deruiter MC, Rensen SS, Coolen GP, Hierck BP, Bergwerff M, Debie WM, Gittenberger-De Groot AC, Van Eys GJ.** Smoothelin expression during chicken embryogenesis: detection of an embryonic isoform. *Dev Dyn* 221: 460–463, 2001.
14. **Dietrich A, Mederos YSM, Gollasch M, Gross V, Storch U, Dubrovska G, Obst M, Yildirim E, Salanova B, Kalwa H, Essin K, Pinkenburg O, Luft FC, Gudermann T, Birnbaumer L.** Increased vascular smooth muscle contractility in TRPC6−/− mice. *Mol Cell Biol* 25: 6980–6989, 2005.
15. **Durvasula RV, Petermann AT, Hiromura K, Blonski M, Pippin J, Mundel P, Pichler R, Griffin S, Couser WG, Shankland SJ.** Activation of a local tissue angiotensin system in podocytes by mechanical strain. *Kidney Int* 65: 30–39, 2004.
16. **Durvasula RV, Shankland SJ.** Mechanical strain increases SPARC levels in podocytes: implications for glomerulosclerosis. *Am J Physiol Renal Physiol* 289: F577–F584, 2005.
17. **Fray TR, Molloy JE, Armitage MP, Sparrow JC.** Quantification of single human dermal fibroblast contraction. *Tissue Eng* 4: 281–291, 1998.
18. **Freichel M, Vennekens R, Olausson J, Stolz S, Philipp S, Weissgerber P, Flockerzi V.** Functional role of TRPC proteins in native systems: implications from knockout and knock-down studies. *J Physiol* 2005.
19. **Giaever I, Keese CR.** A morphological biosensor for mammalian cells. *Nature* 366: 591–592, 1993.
20. **Gloy J, Henger A, Fischer KG, Nitschke R, Mundel P, Bleich M, Schollmeyer P, Greger R, Pavenstadt H.** Angiotensin II depolarizes podocytes in the intact glomerulus of the Rat. *J Clin Invest* 99: 2772–2781, 1997.
21. **Kataoka N, Iwaki K, Hashimoto K, Mochizuki S, Ogasawara Y, Sato M, Tsujioka K, Kajiya F.** Measurements of endothelial cell-to-cell and cell-to-substrate gaps and micromechanical properties of endothelial cells during monocyte adhesion. *Proc Natl Acad Sci USA* 99: 15638–15643, 2002.
22. **Kestila M, Lenkkeri U, Mannikko M, Lamerdin J, McCready P, Putaala H, Ruotsalainen V, Morita T, Nissinen M, Herva R, Kashtan CE, Peltonen L, Holmberg C, Olsen A, Tryggvason K.** Positionally cloned gene for a novel glomerular protein—nephrin—is mutated in congenital nephrotic syndrome. *Mol Cell* 1: 575–582, 1998.
23. **Khodarev NN, Yu J, Nodzenski E, Murley JS, Kataoka Y, Brown CK, Grdina DJ, Weichselbaum RR.** Method of RNA purification from endothelial cells for DNA array experiments. *Biotechniques* 32: 316, 318, 320, 2002.
24. **Kobayashi N.** Mechanism of the process formation; podocytes vs. neurons. *Microsc Res Tech* 57: 217–223, 2002.
25. **Kramer J, Aguirre-Arteta AM, Thiel C, Gross CM, Dietz R, Cardoso MC, Leonhardt H.** A novel isoform of the smooth muscle cell differentiation marker smoothelin. *J Mol Med* 77: 294–298, 1999.
26. **Lewko B, Bryl E, Witkowski JM, Latawiec E, Golos M, Endlich N, Hahnel B, Koksch C, Angielski S, Kriz W, Stepinski J.** Characterization of glucose uptake by cultured rat podocytes. *Kidney Blood Press Res* 28: 1–7, 2005.
27. **Loutzenhiser R, Bidani A, Chilton L.** Renal myogenic response: kinetic attributes and physiological role. *Circ Res* 90: 1316–1324, 2002.
28. **Luimula P, Ahola H, Wang SX, Solin ML, Aaltonen P, Tikkanen I, Kerjaschki D, Holthofer H.** Nephrin in experimental glomerular disease. *Kidney Int* 58: 1461–1468, 2000.
29. **Morton MJ, Hutchinson K, Mathieson PW, Witherden IR, Saleem MA, Hunter M.** Human podocytes possess a stretch-sensitive, Ca^{2+}-activated K^+ channel: potential implications for the control of glomerular filtration. *J Am Soc Nephrol* 15: 2981–2987, 2004.
30. **Mundel P, Kriz W.** Structure and function of podocytes: an update. *Anat Embryol (Berl)* 192: 385–397, 1995.
31. **Mundel P, Reiser J, Zuniga Mejia Borja A, Pavenstadt H, Davidson GR, Kriz W, Zeller R.** Rearrangements of the cytoskeleton and cell contacts induce process formation during differentiation of conditionally immortalized mouse podocyte cell lines. *Exp Cell Res* 236: 248–258, 1997.
32. **Neal CR, Crook H, Bell E, Harper SJ, Bates DO.** Three-dimensional reconstruction of glomeruli by electron microscopy reveals a distinct restrictive urinary subpodocyte space. *J Am Soc Nephrol* 16: 1223–1235, 2005.
33. **Niessen P, Clement S, Fontao L, Chaponnier C, Teunissen B, Rensen S, van Eys G, Gabbiani G.** Biochemical evidence for interaction between smoothelin and filamentous actin. *Exp Cell Res* 292: 170–178, 2004.
34. **Pavenstadt H, Kriz W, Kretzler M.** Cell biology of the glomerular podocyte. *Physiol Rev* 83: 253–307, 2003.
35. **Peppiatt CM, Howarth C, Mobbs P, Attwell D.** Bidirectional control of CNS capillary diameter by pericytes. *Nature* 443: 700–704, 2006.
36. **Rastaldi MP, Armelloni S, Berra S, Calvaresi N, Corbelli A, Giardino LA, Li M, Wang GQ, Fornasieri A, Villa A, Heikkila E, Soliymani R, Boucherot A, Cohen CD, Kretzler M, Nitsche A, Ripamonti M, Malgaroli A, Pesaresi M, Forloni GL, Schlondorff D, Holthofer H, D'Amico G.** Glomerular podocytes contain neuron-like functional synaptic vesicles. *FASEB J* 20: 976–978, 2006.
37. **Reiser J, Kriz W, Kretzler M, Mundel P.** The glomerular slit diaphragm is a modified adherens junction. *J Am Soc Nephrol* 11: 1–8, 2000.
38. **Reiser J, Polu KR, Moller CC, Kenlan P, Altintas MM, Wei C, Faul C, Herbert S, Villegas I, Avila-Casado C, McGee M, Sugimoto H, Brown D, Kalluri R, Mundel P, Smith PL, Clapham DE, Pollak MR.** TRPC6 is a glomerular slit diaphragm-associated channel required for normal renal function. *Nat Genet* 37: 739–744, 2005.

39. **Rensen SS, Niessen PM, Long X, Doevendans PA, Miano JM, van Eys GJ.** Contribution of serum response factor and myocardin to transcriptional regulation of smoothelins. *Cardiovasc Res* 70: 136–145, 2006.

40. **Saleem MA, Ni L, Witherden I, Tryggvason K, Ruotsalainen V, Mundel P, Mathieson PW.** Co-localization of nephrin, podocin, and the actin cytoskeleton: evidence for a role in podocyte foot process formation. *Am J Pathol* 161: 1459–1466, 2002.

41. **Saleem MA, O'Hare MJ, Reiser J, Coward RJ, Inward CD, Farren T, Xing CY, Ni L, Mathieson PW, Mundel P.** A conditionally immortalized human podocyte cell line demonstrating nephrin and podocin expression. *J Am Soc Nephrol* 13: 630–638, 2002.

42. **Saxen L, Sariola H.** Early organogenesis of the kidney. *Pediatr Nephrol* 1: 385–392, 1987.

43. **Shih NY, Li J, Karpitskii V, Nguyen A, Dustin ML, Kanagawa O, Miner JH, Shaw AS.** Congenital nephrotic syndrome in mice lacking CD2-associated protein. *Science* 286: 312–315, 1999.

44. **Takahashi K, Yoshimoto R, Fuchibe K, Fujishige A, Mitsui-Saito M, Hori M, Ozaki H, Yamamura H, Awata N, Taniguchi S, Katsuki M, Tsuchiya T, Karaki H.** Regulation of shortening velocity by calponin in intact contracting smooth muscles. *Biochem Biophys Res Commun* 279: 150–157, 2000.

45. **Tusher VG, Tibshirani R, Chu G.** Significance analysis of microarrays applied to the ionizing radiation response. *Proc Natl Acad Sci USA* 98: 5116–5121, 2001.

46. **Van der Loop FT, Schaart G, Timmer ED, Ramaekers FC, van Eys GJ.** Smoothelin, a novel cytoskeletal protein specific for smooth muscle cells. *J Cell Biol* 134: 401–411, 1996.

47. **Wang Z, Wang DZ, Hockemeyer D, McAnally J, Nordheim A, Olson EN.** Myocardin and ternary complex factors compete for SRF to control smooth muscle gene expression. *Nature* 428: 185–189, 2004.

48. **Wang Z, Wang DZ, Pipes GC, Olson EN.** Myocardin is a master regulator of smooth muscle gene expression. *Proc Natl Acad Sci USA* 100: 7129–7134, 2003.

49. **Watanabe M, Layne MD, Hsieh CM, Maemura K, Gray S, Lee ME, Jain MK.** Regulation of smooth muscle cell differentiation by AT-rich interaction domain transcription factors Mrf2alpha and Mrf2beta. *Circ Res* 91: 382–389, 2002.

50. **Winn MP, Conlon PJ, Lynn KL, Farrington MK, Creazzo T, Hawkins AF, Daskalakis N, Kwan SY, Ebersviller S, Burchette JL, Pericak-Vance MA, Howell DN, Vance JM, Rosenberg PB.** A mutation in the TRPC6 cation channel causes familial focal segmental glomerulosclerosis. *Science* 308: 1801–1804, 2005.

51. **Worth NF, Rolfe BE, Song J, Campbell GR.** Vascular smooth muscle cell phenotypic modulation in culture is associated with reorganization of contractile and cytoskeletal proteins. *Cell Motil Cytoskeleton* 49: 130–145, 2001.

52. **Wrobel LK, Fray TR, Molloy JE, Adams JJ, Armitage MP, Sparrow JC.** Contractility of single human dermal myofibroblasts and fibroblasts. *Cell Motil Cytoskeleton* 52: 82–90, 2002.

53. **Yoshida T, Kawai-Kowase K, Owens GK.** Forced expression of myocardin is not sufficient for induction of smooth muscle differentiation in multipotential embryonic cells. *Arterioscler Thromb Vasc Biol* 24: 1596–1601, 2004.

54. **Yoshida T, Sinha S, Dandre F, Wamhoff BR, Hoofnagle MH, Kremer BE, Wang DZ, Olson EN, Owens GK.** Myocardin is a key regulator of CArG-dependent transcription of multiple smooth muscle marker genes. *Circ Res* 92: 856–864, 2003.

55. **Zavadil J, Cermak L, Soto-Nieves N, Bottinger EP.** Integration of TGF-beta/Smad and Jagged1/Notch signalling in epithelial-to-mesenchymal transition. *EMBO J* 23: 1155–1165, 2004.